Proc. Natl. Acad. Sci. USA
Vol. 87, pp. 6718–6722, September 1990
Neurobiology

Biophysical model of a Hebbian synapse

(long-term potentiation/Hebb's postulate/neuronal plasticity/Ca^{2+} dynamics/spines)

ANTHONY ZADOR*, CHRISTOF KOCH†, AND THOMAS H. BROWN*‡

*Department of Psychology, Yale University, New Haven, CT 06520; and †Computation and Neural Systems Program, California Institute of Technology, Pasadena, CA 91125

Communicated by Francis Crick, May 25, 1990

ABSTRACT **We present a biophysical model of electrical and Ca^{2+} dynamics following activation of *N*-methyl-D-aspartate (NMDA) receptors located on a dendritic spine. The model accounts for much of the phenomenology of the induction of long-term potentiation at a Hebbian synapse in hippocampal region CA1. Computer simulations suggested four important functions of spines in this Ca^{2+}-dependent synaptic modification: (*i*) compartmentalizing transient changes in $[Ca^{2+}]$ to just those synapses that satisfy the conjunctive requirement for synaptic modification; (*ii*) isolating the spine head from changes in the $[Ca^{2+}]$ at the dendritic shaft; (*iii*) amplifying the concentration changes at those synapses; and (*iv*) increasing the voltage dependence of the processes underlying long-term potentiation induction. This proposed role of spines in the regulation of Ca^{2+} dynamics contrasts with traditional approaches to spine function that have stressed electrotonic properties. This model can be used to explore the computational implications of Hebbian synapses.**

Long-term potentiation (LTP) is a persistent synaptic enhancement that can be induced by brief periods of synaptic activity. It is a leading candidate for a synaptic mechanism of rapid learning in mammals. The induction of one form of hippocampal LTP requires the conjunction of presynaptic stimulation with a sufficient level of postsynaptic depolarization (1–3). This interaction between pre- and postsynaptic activity has been interpreted (4) as a biological instance of the type of synapse that Hebb (5) postulated to underlie learning. Theoretical studies have revealed that networks of simple processing elements connected by Hebbian synapses can exhibit powerful forms of learning and self-organization (6–8; for review, see ref. 4).

The biophysical basis of LTP has been the subject of intensive research (for reviews, see refs. 9–11). The induction of one form of LTP requires an increase in the $[Ca^{2+}]$ at a postsynaptic site (12, 13). This increase is thought to be mediated by Ca^{2+} influx through the *N*-methyl-D-aspartate (NMDA) receptor-gated channel (13, 14). Because the channel requires both ligand binding and postsynaptic depolarization for activation, it is ideally suited to contribute to the interactive requirement (4) for a Hebbian synapse.

We have been interested in the role of the dendritic spine in LTP induction (9, 11, 15) and have constructed a biophysical model of electrical and Ca^{2+} dynamics in a spine after activation of NMDA receptors. Computer simulations indicate that the model can account for much of the known phenomenology of LTP induction at a Hebbian synapse in the CA1 region of the hippocampus. The results suggest that the microphysiology of the spine plays a critical role in the induction of this form of LTP.

The publication costs of this article were defrayed in part by page charge payment. This article must therefore be hereby marked "*advertisement*" in accordance with 18 U.S.C. §1734 solely to indicate this fact.

MODEL

The biophysical mechanism of LTP induction has been best studied at the Schaffer collateral/commissural inputs to pyramidal cells of the CA1 region of the rodent hippocampus in the *in vitro* brain slice preparation. At least two pharmacologically distinguishable receptors mediate the excitatory postsynaptic response in this system. NMDA receptors mediate a slow current (16) with a substantial Ca^{2+} component. The associated channel is voltage-dependent due to block by Mg^{2+} that is relieved by membrane depolarization (17–19). Non-NMDA receptors mediate a more rapid current with a negligible Ca^{2+} component.

We simulated Ca^{2+} influx, transport, and buffering following activation of NMDA receptor-gated channels located on a spine head. The model (Fig. 1) consisted of separate electrical and Ca^{2+} components (15). The equations describing electrical and chemical dynamics were advanced independently and at the end of each time step electrical current was converted to ionic flux through Faraday's constant. These equations were discretized and then solved using alternating implicit–explicit steps (20, 21).

Spine and Synapse. Total synaptic current (Fig. 1) was the sum of separate NMDA and non-NMDA components. An alpha function (22),

$$I(t) = (E_{syn} - V_m)\, \kappa g_p t \exp(-t/t_p), \qquad [1]$$

was used for the non-NMDA current, with $\kappa = e/t_p$, e the base of the natural logarithm, $t_p = 1.5$ msec, $E_{syn} = 0$ mV, and the peak conductance $g_p = 0.5$ nS (9, 23). The NMDA conductance was a function of both time and membrane potential. The voltage-dependence was derived from a model in which the binding rate constant of Mg^{2+} to the site of channel block varied as a function of voltage (17, 24). Specifically,

$$I(t) = (E_{syn} - V_m) g_n \frac{\exp(-t/\tau_1) - \exp(-t/\tau_2)}{1 + \eta\,[\mathrm{Mg}]\exp(-\gamma V)}, \qquad [2]$$

with $\tau_1 = 80$ msec, $\tau_2 = 0.67$ msec, $\eta = 0.33$/mM, $\gamma = 0.06$/mV, $E_{syn} = 0$ mV, and $g_n = 0.2$ nS. These parameters were based on voltage-clamp studies of synaptic currents in the hippocampal slice (25) and on single-channel recordings from cultured hippocampal neurons (24). Short trains of synaptic stimulations were modeled as the sum of these conductance waveforms.

Neuronal Structure. To explore the spatiotemporal interactions between inputs, we constructed a simplified model of a whole hippocampal neuron. The neuronal structure consisted of a bifurcating apical branch and a single basal branch emerging from the soma (cf. ref. 26). The following electrical parameters were used: $R_m = 20$ kΩ·cm^2, $R_i = 100$ Ω·cm,

Abbreviations: LTP, long-term potentiation; NMDA, *N*-methyl-D-aspartate; CaM, calmodulin.

‡To whom reprint requests should be addressed.

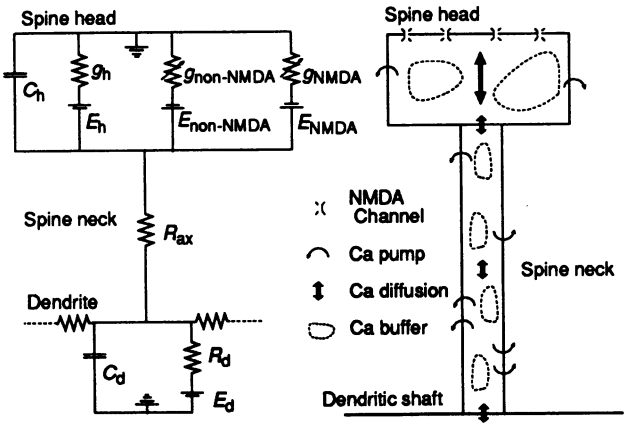

FIG. 1. The model. The electrical model (*Left*) of the spine included two separate conductances representing the distinct NMDA (Eq. 2) and non-NMDA (Eq. 1) components of the synaptic response. The dendritic compartment was connected to 27 other compartments representing the rest of the neuron. In the Ca^{2+} transport-buffering model (*Right*), Ca^{2+} entered the spine head through channels located only on the distal spine head and then diffused along the length of the spine to the dendritic shaft. Diffusion was limited by binding to saturable membrane pumps and cytosolic buffers.

and $C_m = 1\ \mu F/cm^2$ (cf. refs. 9, 27), where R_m is membrane resistance, R_i is intracellular resistivity, and C_m is membrane capacitance. Unless otherwise stated, a single synapse was placed on the head of a spine located half-way between the soma and the termination of the longer apical branch. The spine axial resistance was 125 MΩ, and the input resistance at the spine head was 200 MΩ.

Calcium-Transport Buffering. Ca^{2+} entered through NMDA receptor-gated channels located on the distal part of a spine head. It then diffused along the length of the spine to the dendritic shaft. Ca^{2+} was also buffered and pumped in each compartment. The $[Ca^{2+}]$ at the shaft was generally fixed at the assumed resting value ($[Ca^{2+}]_{rest} = 0.05\ \mu M$), although in some simulations it was fixed at a higher value (1.0 μM; see *Isolation* below). For purposes of Ca^{2+} transport and buffering (Fig. 1), the spine geometry was modeled as a short cylindrical head at the end of a long cylindrical neck. The following radii (r) and lengths (l) were used: $r_{neck} = 0.05\ \mu m$, $l_{neck} = 1.0\ \mu m$; $r_{head} = 0.25\ \mu m$, $l_{head} = 0.30\ \mu m$. We solved the one-dimensional diffusion equation with $D = 0.6\ \mu m^2/msec$, using a discretization of 0.1 μm per compartment. The diffusion equation represents the continuum limit of an isotropic random walk. Although this continuum approximation is adequate at the high $[Ca^{2+}]$ upon which the conclusions in this paper are based, it may introduce a small error at the resting $[Ca^{2+}]$, at which only about two calcium ions are free in the spine head.

At membrane voltages substantially more positive than the synaptic reversal potential (≈0 mV) there is no inward Ca^{2+} flux, even when the Ca^{2+} equilibrium potential is substantially higher (13, 28). Ionic current through the NMDA receptor-gated channel was assumed unidirectional, rather than the sum of independent outward and inward components. A fixed fraction (0.02) of the inward current was assumed to be carried by Ca^{2+} (C. F. Stevens, personal communication). We neglected small changes in E_{syn} arising from changes in the concentrations of permeant cations (cf. ref. 29).

There is little quantitative evidence regarding the density and properties of Ca^{2+} pumps in mammalian brain neurons. Reported densities range from $1 \times 10^{-14}\ \mu mol/\mu m^2$ in sarcoplasmic reticulum—one-fifth the maximum theoretical membrane density of a protein that size (30)—to $4 \times 10^{-16}\ \mu mol/\mu m^2$ in squid axon. We modeled two separate pumps for Ca^{2+} extrusion from the spine lumen. Both obeyed saturable first-order Michaelis–Menton kinetics:

$$\frac{\partial[Ca]_{pump}}{\partial t} = -K_{max} P_s \frac{A}{V} \frac{[Ca]}{[Ca] + K_d} + J_{leak} \frac{A}{V}, \quad [3]$$

where $K_{max} = 0.2/msec$ is the Ca^{2+} turnover rate, P_s is the surface density, A/V is the ratio of surface area to volume, J_{leak} is the leak flux of Ca^{2+}, and K_d is the dissociation constant. A higher-affinity ($K_d = 0.5\ \mu M$) lower-capacity pump was included at a uniform density ($P_s = 5 \times 10^{-16}\ \mu mol/\mu m^2$) throughout the spine membrane. The density of a lower-affinity ($K_d = 20\ \mu M$) higher-capacity pump was nonuniform. The density was lower ($P_s = 1 \times 10^{-15}\ \mu mol/\mu m^2$) in the distal one-third of the spine neck and in the spine head than in the rest of the spine neck ($P_s = 5 \times 10^{-15}\ \mu mol/\mu m^2$). The higher density at the base of the spine neck reflects the contribution of the spine apparatus (31, 32), which may be rich in pump molecules. The leak flux (J_{leak}) was determined by setting the net flux due to the pump to 0 at $[Ca^{2+}]_{rest}$.

Calmodulin (CaM) is present at high concentrations at the postsynaptic density, and it has been suggested that a Ca^{2+}-CaM-dependent protein kinase, CaMKII, may be important in LTP induction (for review, see ref. 33). We included in our model a fixed concentration (100.0 μM) of an immobile saturable buffer with a kinetic scheme based on one proposed for CaM (cf. ref. 15). Ca^{2+} binding to four equivalent sites ($k_F = 0.05/\mu M$ per msec and $k_R = 0.5/msec$) was assumed to be sequential and noncooperative. To simplify discussion, we assumed here that the amount of synaptic enhancement depends upon the peak [CaM-Ca_4]. However, many other measures of CaM-Ca_4 activity (such as its time integral), or even measures of other Ca^{2+}-dependent enzymatic processes, gave qualitatively similar results. The critical assumption is that the relation between the $[Ca^{2+}]$ and the amount or probability of LTP is monotonic.

RESULTS

Compartmentalization. The microphysiology of the spine restricted transient changes in $[Ca^{2+}]$ to the spine. During a brief train of synaptic stimuli, the Ca^{2+} influx caused a much greater change in $[Ca^{2+}]$ at the spine head than at the dendrite. This compartmentalization depended primarily upon the shape of the spine and the distribution of pumps. The slender spine neck slowed diffusion, and its high ratio of surface area to volume enhanced the effectiveness of membrane pumps. For our standard parameters, the $[Ca^{2+}]$ in the spine head increased from its resting value of 0.05 μM to almost 10 μM, while at the dendrite it increased only to 0.06 μM (Fig. 2 *Left*). Compartmentalization of activated CaM (Fig. 2 *Right*) was even more pronounced. Because each spine maintains its own microenvironment distinct from that of neighboring spines, synaptic enhancement can be highly selective.

Amplification. In our simulations, even the small Ca^{2+} current through NMDA receptor-gated channels (2% of total current) produced a large change in concentration if the site of influx was at the spine head. This amplification depended primarily upon the restriction of Ca^{2+} to the small volume of the subsynaptic compartment. In simulations of synaptic channels placed directly on a larger dendritic process ($r = 0.5\ \mu m$), the change in $[Ca^{2+}]$ was more than an order of magnitude smaller than at our reference spine head. This amplification may help achieve a $[Ca^{2+}]$ high enough for the induction of LTP. The peak $[Ca^{2+}]$ attained at the spine head during a train of synaptic stimuli was sensitive to assumptions about Ca^{2+} extrusion and buffering. Depending on the choice

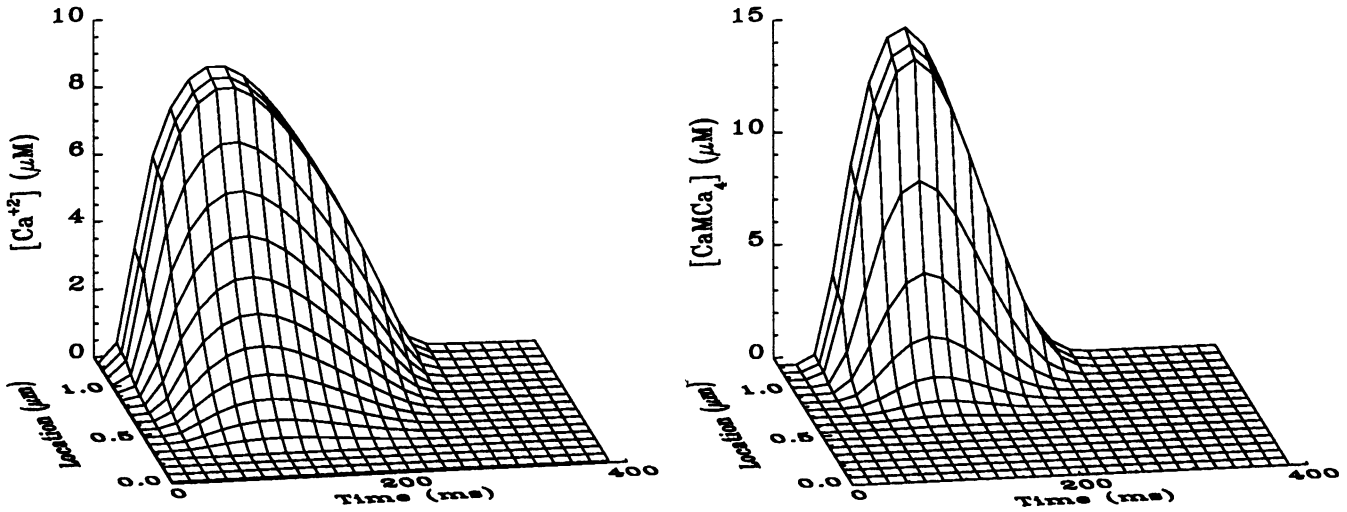

FIG. 2. Spatiotemporal dynamics of Ca^{2+} and CaM-Ca_4. The time course of [Ca^{2+}] (*Left*) and [CaM-Ca_4] (*Right*) in a spine is shown. The axis labeled location indicates distance from dendritic shaft. A train of three presynaptic stimuli was applied at 100 Hz while postsynaptic voltage at the spine head was clamped to −40 mV. Changes in [Ca^{2+}] and [CaM-Ca_4] are restricted mainly to the spine head, where they are amplified. Note that the response of [CaM-Ca_4] is sharper than that of [Ca^{2+}].

of parameters, the peak [Ca^{2+}] ranged from <1 μM to >100 μM. Ca^{2+} dynamics at the dendrite, by contrast, were determined primarily by diffusion. Over the same parameter range, peak dendritic [Ca^{2+}] never exceeded 2 μM. By permitting exquisite regulation of Ca^{2+} dynamics, the spine microphysiology might provide a mechanism for adaptive control of the rate of synaptic modification.

Isolation. Postsynaptic depolarization without presynaptic stimulation does not lead to the induction of LTP in the CA1 region (1). Heterosynaptic LTP is not observed in these synapses (for reviews, see refs. 4, 11). If an increase in [Ca^{2+}] is sufficient to induce LTP, then there is an apparent paradox: Why is Ca^{2+} influx through dendritic Ca^{2+} channels opened during prolonged postsynaptic depolarization not sufficient to induce LTP? One possibility (34) is that the pumps in the spine neck *isolate* the spine head from changes in [Ca^{2+}] at the dendritic shaft. This hypothesis was tested by stepping the dendritic [Ca^{2+}] to an elevated constant value (1 μM). At our reference pump density, the spine head remained protected from this sustained change in dendritic [Ca^{2+}]. This protection may explain the absence of heterosynaptic LTP at these synapses. In the steady state, chemical isolation of the spine head was due to the pumps rather than the saturable buffering system. The buffers affected the rate at which the steady-state [Ca^{2+}] was achieved at the spine head but did not affect its final value.

Coactivity. The Hebbian nature of LTP at the Schaffer collateral/commissural inputs to pyramidal cells in the CA1 region is one of the best documented and least controversial results in LTP research. In our model, this coactivity requirement (Fig. 3) arose from the voltage dependence of the NMDA receptor-gated channel (Eq. 2) and from the nonlinear relationship between synaptic current and peak [Ca^{2+}] at the spine head. The peak concentration of activated CaM during synaptic input increased from 1.8×10^{-3} μM at −80 mV to 20 μM at −30 mV (Fig. 3 *Top*). While the details of the voltage dependence shown in Fig. 3 depended on our assumptions about spine microphysiology, LTP induction retained its requirement for conjunctive activity—the defining feature of Hebbian LTP—over a very wide range of parameter values.

The requirement for postsynaptic depolarization may be satisfied through coactive synaptic input. In the associative paradigm for LTP induction, a weak input that is not in itself capable of inducing LTP when presented alone is potentiated when paired with a strong input (35, 36). In these simulations, the strong input was modeled as simultaneous activation of synapses distributed uniformly on the same apical dendrite as the spine. The conductance change at each strong input

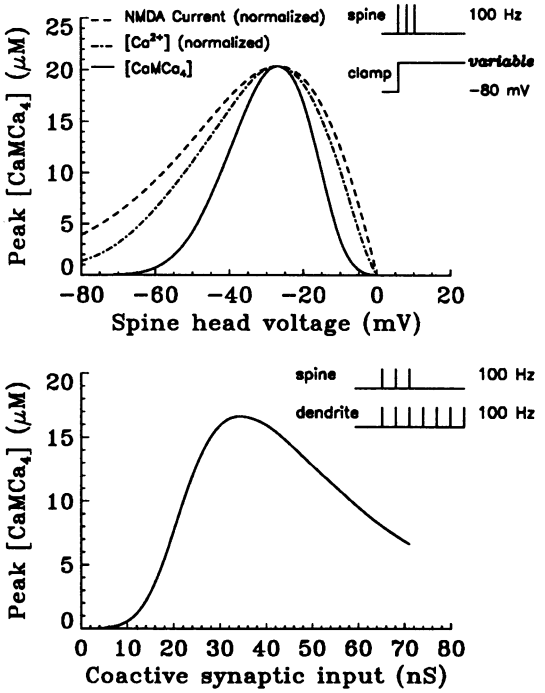

FIG. 3. Effect of postsynaptic activity. Peak [CaM-Ca_4] in the subsynaptic compartment is shown after a train of three presynaptic stimuli applied at 100 Hz. In the first type of simulation, the postsynaptic membrane was clamped to potentials ranging from −80 mV to 0 mV (*Top*). Peak [Ca^{2+}] and NMDA current have been scaled to this graph. Note that [Ca^{2+}] and [CaM-Ca_4] are steeper functions of voltage than NMDA current. In the second kind of simulation, postsynaptic depolarization was provided by a coactive strong input (*Bottom*). The strong input consisted of a 100 Hz train of stimuli applied at synapses uniformly distributed on the same apical branch as the spine. The strength of the strong input stimulus, defined as peak total conductance of the coactive synapses, was varied from 0 nS to 75 nS. Note that for very low values of strong input activity (only weak input; see text), peak [CaM-Ca_4] remains essentially unchanged from the resting value of [CaM-Ca_4].

synapse was given by Eqs. 1 and 2. We also simulated the limiting case of a weak input: activity at a single synapse. A train of weak stimuli alone did not result in a substantial increase in [CaM-Ca_4], whereas in conjunction with strong input stimuli there was a large increase (Fig. 3 *Bottom*). In these simulations, a concomitant strong input of ≈10 nS or greater was required for the induction of LTP (Fig. 3 *Bottom*).

It is noteworthy that a weak stimulus alone did not induce LTP in these simulations. It has been proposed (37, 38) that if NMDA receptors were colocalized with non-NMDA receptors on the spine head (23) as in the present model, then even a weak input would provide sufficient depolarization at the spine head for the induction of LTP. According to this argument, NMDA receptors must, therefore, be located on the dendritic shaft. The depolarization at the spine head due to a single input, however, depends on the size of the peak synaptic conductance change, g_p. If g_p were large (≈10 nS), then indeed the depolarization of the spine head in response to a single synaptic input would be sufficient for the induction of LTP. Although the actual value of g_p has not been determined precisely, it appears much smaller (≤ 1 nS; cf. refs. 9, 23) than others have assumed. Because this small g_p does not result in sufficient depolarization at the spine head, a weak input is potentiated only if coupled with a strong input.

Voltage Dependence. The Ca^{2+} transport-buffering system in the spine may increase the voltage dependence of the processes underlying LTP induction. The voltage dependence that we have assumed for the NMDA receptor-gated channel is not very steep (Fig. 3 *Top*). The current at −80 mV was only 4.4 times less than at −40 mV. Both [Ca^{2+}] and the concentration of activated CaM varied as steeper functions of voltage than the NMDA current following a given number of stimuli. At hyperpolarized voltages, where the NMDA-mediated Ca^{2+} current remained small, [Ca^{2+}] was kept below the K_d (0.5 μM) of the higher-affinity lower-capacity pump. As this pump system approached saturation, increased Ca^{2+} current due to further depolarization caused [Ca^{2+}] to rise quickly, until activation of the lower-affinity higher-capacity pump slowed the rate of rise. The voltage dependence of peak [CaM-Ca_4] was even steeper than that of [Ca^{2+}]. Nonlinearities in the Ca^{2+} transport-buffering system mapped a 5-fold change in Ca^{2+} current to a 1000-fold range of [CaM-Ca_4] (Fig. 3; cf. ref. 15).

Trace Period. The slow decay of the NMDA current (16) might be an important determinant of the temporal contiguity required between presynaptic activation and postsynaptic depolarization. The persistence of the current is thought to arise from slow unbinding of glutamate from the NMDA receptor. If the synapse is depolarized while neurotransmitter is still bound to the receptor, the channel can open to allow an influx of Ca^{2+}. This suggests that LTP induction should occur even if there is a small temporal gap or "trace period" between the end of presynaptic stimulation and the onset of a sufficiently strong depolarization (11). Fig. 4 illustrates that this trace period may last longer than 40 msec. This prediction of the model may explain a number of experimental observations regarding the induction of LTP by sequential synaptic inputs (11, 39, 40).

Antidromic Spike Invasion. The induction of LTP does not *require* sodium action potentials (1). In our simulations, the depolarization at the subsynaptic membrane due to a postsynaptic train of fast somatic sodium action potentials was not *sufficient*, when paired with a weak presynaptic stimulus, to induce LTP. However, the results were quite different when a uniform density of low-threshold dendritic Ca^{2+} channels (41) was included in the model. Under these conditions, fast somatic action potentials activated the slower dendritic Ca^{2+} currents. The depolarization mediated by these dendritic Ca^{2+} channels in response to somatic Na^+ spikes was sufficient, when paired with a weak stimulus, for the induction of LTP. An experimental question with important theoretical implications is the extent to which back-propagating electrical activity (42) can supply the depolarization required for the induction of LTP.

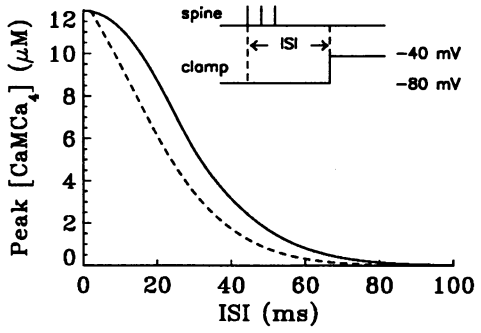

FIG. 4. Effects of the interval between onset of presynaptic stimulation and onset of postsynaptic activity (ISI). Peak [CaM-Ca_4] in the subsynaptic compartment is shown as a function of delay in the onset of postsynaptic activity. A train of three presynaptic stimuli was applied at 100 Hz. The postsynaptic activity consisted of either voltage clamp to −40 mV (——) or a strong input of 25 nS (---). The long time course of the NMDA conductance allows stimuli separated by a substantial ISI to interact.

DISCUSSION

The present biophysical model accounted for the known phenomenology of LTP induction at the Schaffer collateral/commissural synapses of the hippocampus. (*i*) It accounted for the Hebbian nature of LTP induction in these synapses. The requirement for conjunctive pre- and postsynaptic activity was an immediate consequence of the properties of the NMDA receptor-gated channel. In agreement with experimental findings, the requisite postsynaptic depolarization could be provided either by a strong coactive synaptic input (35, 36) or by direct manipulation of membrane potential (1). (*ii*) The model accounted for the input specificity (1, 36) of LTP. The microphysiology of the spine restricted LTP induction to just those synapses that satisfied the conjunctive requirement. (*iii*) The model was consistent with experimentally observed temporal contiguity requirements (39, 40) for LTP induction. Not included in the current model were other forms of synaptic plasticity—such as posttetanic potentiation (11) and synaptic depression (43, 44)—that have also been reported in the Schaffer collateral/commissural synapses.

Simulations of the model suggested four ways in which spines may regulate Ca^{2+} dynamics during the induction of LTP. (*i*) The spine compartmentalized changes in the [Ca^{2+}] to the neighborhood of a single synapse. This compartmentalization could contribute to the input specificity of LTP in the CA1 region. (*ii*) The spine amplified small ionic fluxes through membrane channels into large changes in ionic concentration. Amplification may help achieve a [Ca^{2+}] high enough for the induction of LTP. (*iii*) The spine isolated the subsynaptic membrane from changes in the [Ca^{2+}] at the dendritic shaft. This effect is consistent with the absence of heterosynaptic LTP in these neurons and the fact that postsynaptic activity alone is not sufficient to induce LTP. (*iv*) The microphysiology of the spine increased the slope of the voltage dependence of the processes underlying LTP induction. Further experimental analysis will be required to determine whether the voltage dependence of LTP induction is greater than can be explained directly by the properties of the NMDA receptor-gated channel.

The present suggestion that spines play a critical role in the regulation of Ca^{2+} dynamics contrasts with the more tradi-

tional approach to spine function that has emphasized electronic effects. One previous proposal (45) is that the large spine axial resistance isolates synapses from electrical activity at the dendritic shaft and at neighboring spines. This idea of electrical isolation is not consistent with theoretical results that predict essentially complete voltage transfer from the dendritic shaft to the spine head (9, 46). Another previous hypothesis is that modulation of the spine axial resistance, possibly through changes in spine neck geometry, mediates changes in synaptic efficacy (cf. refs. 47, 48) underlying the expression of hippocampal LTP (49, 50). The extent to which axial resistance can, in fact, control synaptic efficacy depends on the ratio of this resistance to the inverse of the peak synaptic conductance (11, 50, 51). Simulations have suggested that this critical ratio may not be sufficiently large to allow significant control of synaptic efficacy in hippocampal neurons (9, 32). It may be appropriate to shift attention to the role of spines in regulating second messengers.

We thank Dr. Francis Crick for useful discussions, Dr. C. F. Stevens for making experimental results available before publication, and Ms. Anna C. Nobre for comments on the manuscript. This research was supported by grants from the Office of Naval Research and the Defense Advanced Research Projects Agency.

1. Kelso, S. R., Ganong, A. H. & Brown, T. H. (1986) *Proc. Natl. Acad. Sci. USA* **83,** 5326–5330.
2. Malinow, R. & Miller, J. P. (1986) *Nature (London)* **320,** 529–530.
3. Wigstrom, H., Gustafsson, B., Huang, Y.-Y. & Abraham, W. C. (1986) *Acta Physiol. Scand.* **126,** 317–319.
4. Brown, T. H., Kairiss, E. W. & Keenan, C. L. (1990) *Annu. Rev. Neurosci.* **13,** 475–511.
5. Hebb, D. O. (1949) *The Organization of Behavior* (Wiley, New York).
6. Anderson, J. A. (1985) in *Synaptic Modification, Neuron Selectivity, and Nervous System Organization*, eds. Levy, W. B., Anderson, J. A. & Lehmkuhle, S. (Erlbaum Assoc., Hillsdale, NJ), pp. 153–173.
7. Hopfield, J. J. (1984) *Proc. Natl. Acad. Sci. USA* **81,** 3088–3092.
8. Kohonen, T. (1989) *Self-Organization and Associative Memory* (Springer, Berlin).
9. Brown, T. H., Chang, V. C., Ganong, A. H., Keenan, C. L. & Kelso, S. R. (1988) in *Long-Term Potentiation: From Biophysics to Behavior*, eds. Landfield, P. W. & Deadwyler, S. A. (Liss, New York), pp. 197–260.
10. Brown, T. H., Chapman, P. F., Kairiss, E. W. & Keenan, C. L. (1988) *Science* **242,** 724–728.
11. Brown, T. H., Ganong, A. H., Kairiss, E. W., Keenan, C. L. & Kelso, S. R. (1989) in *Neural Models of Plasticity*, eds. Byrne, J. H. & Berry, W. O. (Academic, San Diego, CA), pp. 266–306.
12. Lynch, G., Larsen, J., Kelso, S., Barrionuevo, G. & Schottler, F. (1983) *Nature (London)* **305,** 719–721.
13. Malenka, R. C., Kauer, J. A., Zucker, R. S. & Nicoll, R. A. (1988) *Science* **242,** 81–84.
14. Collingridge, G. L., Kehl, S. J. & McLennan, H. (1983) *J. Physiol. (London)* **334,** 19–31.
15. Gamble, E. & Koch, C. (1987) *Science* **236,** 1311–1315.
16. Forsythe, I. D. & Westbrook, G. L. (1988) *J. Physiol. (London)* **396,** 515–533.
17. Ascher, P. & Nowak, L. (1988) *J. Physiol. (London)* **399,** 247–266.
18. Jahr, C. E. & Stevens, C. F. (1987) *Nature (London)* **325,** 522–525.
19. Cull-Candy, S. G. & Usowicz, M. M. (1987) *Nature (London)* **325,** 525–528.
20. Hines, M. (1984) *Int. J. Bio-Med. Comp.* **15,** 69–76.
21. Mascagni, M. V. (1989) in *Methods in Neuronal Modeling: From Synapses to Networks*, eds. Koch, C. & Segev, I. (MIT Press, Cambridge, MA), pp. 439–484.
22. Brown, T. H. & Johnston, D. (1983) *J. Neurophysiol.* **50,** 487–507.
23. Bekkers, J. M. & Stevens, C. F. (1989) *Nature (London)* **341,** 230–233.
24. Jahr, C. E. & Stevens, C. F. (1990) *J. Neurosci.* **10,** 1830–1837.
25. Nobre, A. C., Xiang, Z., Zador, A. M. & Brown, T. H. (1990) *Soc. Neurosci. Abstr.*, in press.
26. Traub, R. D. (1982) *Neuroscience* **7,** 1233–1242.
27. Brown, T. H., Fricke, R. A. & Perkel, D. H. (1981) *J. Neurophysiol.* **46,** 812–827.
28. MacDermott, A. B., Mayer, M. L., Westbrook, G. L., Smith, S. J. & Barker, J. L. (1986) *Nature (London)* **321,** 519–522.
29. Qian, N. & Sejnowski, T. J. (1989) *Biol. Cybern.* **62,** 1–15.
30. Hille, B. (1984) *Ionic Channels of Excitable Membranes* (Sinauer, Sunderland, MA).
31. Harris, K. M., Jensen, F. E. & Tsao, B. H. (1989) in *The Hippocampus—New Vistas*, eds. Chan-Palay, V. & Kohler, C. (Liss, New York), pp. 32–52.
32. Harris, K. M. & Stevens, J. K. (1989) *J. Neurosci.* **9,** 2982–2997.
33. Kennedy, M. B. (1989) *Cell* **59,** 777–787.
34. Regehr, W. G., Connor, J. A. & Tank, D. W. (1989) *Nature (London)* **341,** 533–536.
35. Barrionuevo, G. & Brown, T. H. (1983) *Proc. Natl. Acad. Sci. USA* **80,** 7347–7351.
36. Kelso, S. R. & Brown, T. H. (1986) *Science* **232,** 85–87.
37. Bliss, T. V. P. & Lynch, M. A. (1988) in *Long-Term Potentiation: From Biophysics to Behavior*, eds. Landfield, P. W. & Deadwyler, S. A. (Liss, New York), pp. 3–72.
38. Wickens, J. (1988) *Prog. Neurobiol.* **31,** 507–528.
39. Steward, O., White, G., Korol, D. & Levy, W. B. (1988) in *Long-Term Potentiation: From Biophysics to Behavior*, eds. Landfield, P. W. & Deadwyler, S. A. (Liss, New York), pp. 139–166.
40. Larsen, J. & Lynch, G. (1989) *Brain Res.* **489,** 49–58.
41. Doerner, D., Pitler, T. A. & Alger, B. E. (1988) *J. Neurosci.* **11,** 4069–4078.
42. Richardson, T. L., Turner, R. W. & Miller, J. J. (1987) *J. Neurophysiol.* **58,** 981–996.
43. Dunwiddie, T. & Lynch, G. (1978) *J. Physiol. (London)* **276,** 353–367.
44. Stanton, P. K. & Sejnowski, T. J. (1989) *Nature (London)* **339,** 215–218.
45. Diamond, J., Gray, E. G. & Yasargil, G. M. (1970) in *Excitatory Synaptic Mechanisms*, eds. Andersen, P. & Jensen, J. K. S. (Universitetsforlaget, Oslo), pp. 213–222.
46. Carnevale, N. T. & Johnston, D. (1982) *J. Neurophysiol.* **47,** 606–621.
47. Chang, H.-T. (1952) *Cold Spring Harbor Symp. Quant. Biol.* **17,** 189–202.
48. Rall, W. (1970) in *Excitatory Synaptic Mechanisms*, eds. Andersen, P. & Jensen, J. K. S. (Universitetsforlaget, Oslo), pp. 175–187.
49. Bliss, T. V. P. & Lomo, T. (1973) *J. Physiol. (London)* **232,** 331–356.
50. Koch, C. & Poggio, T. (1983) *Proc. R. Soc. Lond. B* **218,** 455–477.
51. Wilson, C. J. (1984) *J. Neurosci.* **4,** 281–297.